



Published in final edited form as:

Am J Ophthalmol. 2019 December ; 208: 1–11. doi:10.1016/j.ajo.2019.06.017.

Two-Year Risk of Exudation in Eyes with Non-Exudative AMD and Subclinical Neovascularization Detected with Swept Source OCT Angiography

Jin Yang^{1,4}, Qinqin Zhang², Elie H. Motulsky¹, Marie Thulliez¹, Yingying Shi¹, Cancan Lyu¹, Luis de Sisternes³, Mary K. Durbin³, William Feuer¹, Ruikang K. Wang², Giovanni Gregori¹, Philip J. Rosenfeld¹

¹Department of Ophthalmology, Bascom Palmer Eye Institute, University of Miami Miller School of Medicine, Miami, Florida

²Department of Bioengineering, University of Washington, Seattle, Washington

³Research and Development, Carl Zeiss Meditec, Inc., Dublin, CA

⁴Tianjin Medical University Eye Hospital, Tianjin, China.

Abstract

Purpose: Swept source optical coherence tomography angiography (SS-OCTA) was used to study the prevalence, incidence, and natural history of subclinical macular neovascularization (MNV) in eyes with unilateral non-exudative age-related macular degeneration (AMD).

Design: Prospective cohort study.

Methods: Patients were imaged using 3×3 mm and 6×6 mm SS-OCTA scan patterns. MNV was detected using the outer retina to choriocapillaris *en face* slab. Prevalence and incidence of subclinical MNV, Kaplan-Meier cumulative estimates for the overall risk of exudation, and the association between neovascular lesion size and the risk of exudation were assessed through 2 years.

Results: From August 2014 through March 2018, 227 patients (154 intermediate and 73 late AMD eyes) underwent SS-OCTA imaging. Thirty eyes (13.2%) had subclinical MNV at first imaging and 12 eyes (8.9%) developed subclinical MNV during follow-up. Of the 191 eyes with more than one visit, 19 developed exudation. Fourteen of these eyes had pre-existing subclinical MNV. The incidence of exudation from the time of first detection of any subclinical MNV was 34.5%. The relative risk of exudation after detection of subclinical MNV was 13.6 times greater (95% confidence interval, 4.9–37.7) than in the absence of subclinical MNV ($P < 0.001$). There was no significant risk of exudation based on lesion size alone ($P = 0.91$).

Corresponding Author: Philip J. Rosenfeld MD, PhD, Bascom Palmer Eye Institute, 900 NW 17th street, Miami, FL, 33136, Phone: 305-326-6148, Fax: 305-326-6538, prosenfeld@miami.edu.

Publisher's Disclaimer: This is a PDF file of an unedited manuscript that has been accepted for publication. As a service to our customers we are providing this early version of the manuscript. The manuscript will undergo copyediting, typesetting, and review of the resulting proof before it is published in its final citable form. Please note that during the production process errors may be discovered which could affect the content, and all legal disclaimers that apply to the journal pertain.

Conclusions: By 24 months, the risk of exudation was 13.6-times greater for eyes with subclinical MNV detected by SS-OCTA compared with eyes without subclinical MNV. For eyes with subclinical MNV in the absence of symptomatic exudation, we recommend close follow-up without treatment.

INTRODUCTION

Exudation from macular neovascularization (MNV) is a feature of late-stage age-related macular degeneration (AMD) and is associated with rapid, severe vision loss unless treated with intravitreal injections of vascular endothelial growth factor (VEGF) inhibitors.^{1,2} However, the onset of exudation does not necessarily coincide with the formation of MNV. In the 1990s, studies showed that indocyanine green angiography (IGGA) could identify MNV in eyes with AMD in the absence of exudation; however, these eyes were at higher risk for developing exudation compared with eyes without detectable MNV.^{3,4}

While ICGA has been used to identify subclinical non-exudative MNV in the past,³⁻⁶ optical coherence tomography angiography (OCTA) has been used more recently to identify these lesions.^{7,8} OCTA is particularly effective in identifying type 1 and type 3 MNV prior to exudation, and swept source OCTA (SS-OCTA) is better at detecting and fully delineating the type 1 MNV compared with spectral domain OCTA (SD-OCTA) imaging.⁹⁻¹¹ SS-OCTA not only identifies these lesions, but also has advantages over routine ICGA for the monitoring of these lesions because it is non-invasive, safer, faster, less expensive to perform, and easily repeated at routine follow-up visits. Moreover, with a single OCTA raster scan, both structure and flow information are obtained, so the onset of exudation can be easily detected from retinal thickness maps or by reviewing individual B-scans.⁸

We previously reported on the prevalence and incidence of subclinical MNV in eyes with non-exudative AMD in which the fellow eye had been diagnosed with exudative AMD.⁷ In 160 eyes with non-exudative AMD, we found that the prevalence of subclinical MNV was 14.4%. The presence of subclinical MNV resulted in a 15.2-fold higher risk of exudation after one-year compared with eyes without detectable MNV. We concluded that SS-OCTA was useful for identifying these subclinical neovascular lesions, and eyes with these subclinical lesions were at much higher risk of exudation. One of the limitations of this previous study was that we only reported on one-year follow-up for these patients.

In this current report, we continued to recruit patients into the study and monitored these patients for a longer period of time to determine the results through two years of follow-up.

METHODS

Patients with exudative AMD in one eye and non-exudative AMD in the fellow eye were enrolled from August 2014 through March 2018 in a prospective, observational and consecutive OCT imaging study at the Bascom Palmer Eye Institute. The institutional review board (IRB) of the University of Miami Miller School of Medicine approved the study and all patients signed an informed consent for this prospective OCT study. The study was performed in accordance with the tenets of the Declaration of Helsinki and complied with the Health Insurance Portability and Accountability Act of 1996.

All eyes in the study underwent SS-OCTA imaging at baseline and during the follow-up period by the same technician. Over the course of this study, three different SS-OCTA prototype instruments were used to image the patients. The differences of these three SS-OCTA prototype instruments were described in the previous report.⁷ The third SS-OCTA instrument (PLEX® Elite 9000; Carl Zeiss Meditec, Inc, Dublin, CA) was used to image our patients since April 2016 and has been cleared by the Food and Drug Administration. This instrument uses a swept laser source with a central wavelength of 1060 nm and a scanning speed of 100,000 A-scans per second. The axial and lateral resolutions of the system were 5 μm in tissue and 14 μm at the retinal surface, respectively. The 3 \times 3 mm scan consisted of 300 A-scans per B scan repeated four times at each of 300 B-scan positions, resulting in a homogeneous sampling grid with 10 μm spacing. The 6 \times 6 mm scan consisted of 500 A-scans per B-scan repeated twice at each of 500 B-scan positions, resulting in a 12 μm separation of A-scans and B-scans. All patients in this study were imaged using the 3 \times 3mm and 6 \times 6mm scan patterns. All scans were centered on the fovea, and FastTrack™ motion correction software (Carl Zeiss Meditec, Inc., Dublin, CA, USA) was used while the images were acquired. Subclinical neovascular lesions not fully contained or outside the 6 \times 6mm field of view were excluded from enrollment in this current study.

Eyes with non-exudative AMD were classified as either intermediate AMD (iAMD) or late AMD according to the previous classification standard.^{7,12} Late AMD was characterized by geographic atrophy (GA). At baseline, the absence of exudation was determined by reviewing individual B-scans to document the absence of intraretinal or subretinal fluid. The accumulation of fluid under the retinal pigment epithelium (RPE) in the absence of subretinal or intraretinal fluid was not considered evidence of exudation. Time to symptomatic exudation in this study was defined by the day the patient received treatment with intravitreal anti-VEGF therapy.

The complex optical microangiographic (OMAG^c) algorithm was used to generate flow information by using variations in both of the OCT signal magnitude and phase information between sequential B-scans acquired at the same position.^{13,14} The boundaries used to identify MNV in this study extended from the outer retina to the choriocapillaris and is referred to as the ORCC slab, which was previously described and validated for the identification of MNV.^{10,15,16} The area measurements of the MNV detected by using the ORCC slab en face flow images were obtained by using a validated automated algorithm with retinal vessel projection artifacts being removed from this ORCC slab as previously described.^{15–18} Color coding of B scans was used to identify flow in different compartments of the macula in order to provide better depth-encoded visualization of the neovascularization.

The area measurements of the subclinical neovascular lesions were performed at baseline and at selected follow-up visits to determine if the size of the MNV correlated with exudation. If a lesion developed exudation, then the last two visits before exudation were measured, and if the lesion did not develop exudation during the follow-up period, then the last two visits prior to the final follow-up visit were measured. To determine if the size of the subclinical MNV could be used to predict the need for anti-VEGF therapy, the neovascular lesion sizes from the last two visits prior to exudation were compared with the neovascular

lesion sizes from the last two visits prior to the final follow-up visit of eyes that did not develop exudation. The area under the receiver operator characteristic curves (AUROC) were estimated to address the sensitivity and specificity of the lesion sizes at the last two visits in their ability to predict exudation. An area of 0.5 suggests there is no ability to discriminate based on the measurement and an area approaching 1.0 (or zero) indicates excellent ability to discriminate. In addition, baseline lesions were split into tertiles based on their size to compare the association between baseline size with the risk of exudation. Since follow up time for the baseline lesion is a factor that affects our ability to analyze the exudation prediction, cumulative rates of incidence of exudation were calculated with the Kaplan-Meier method and compared using different baseline lesion size groups with the log-rank test. The method of calculating and comparing the cumulative rates of incident exudation and the ratio of the exudation risk with or without subclinical MNV was the same method used in our previous one year study.⁷ The ratio of exudation risk with or without subclinical MNV was estimated with a Cox proportional hazards survival analysis in which the observation of subclinical MNV was included as a time-dependent covariate.

RESULTS

A total of 227 patients with exudative AMD in one eye and non-exudative AMD in the fellow eye were enrolled from August 2014 through March 2018. Of the 227 eyes with non-exudative AMD, 154 eyes (68%) were diagnosed with iAMD (61.0% women) and 73 eyes (32%) were diagnosed with late AMD (60.3% women). Overall, ages ranged from 50 to 101 years old with a mean age of 79.8 years. The mean ages of the iAMD group and late AMD groups were 78.7 years old and 82.2 years old, respectively.

Prevalence and Natural History

At the time of first SS-OCTA imaging, subclinical MNV was identified in 30 of 227 eyes, for a prevalence of 13.2%. In the eyes with non-exudative AMD, subclinical MNV was found in 19 eyes with iAMD (12.3%), and in 11 eyes with late AMD (15.1%. $P=0.675$, Fisher exact test). Of the 30 eyes in which a subclinical MNV was identified at first SS-OCTA imaging, all the lesions were classified as type 1 MNV.

A total of 191 eyes had follow-up visits. Of these 191 eyes, 127 (66%) were diagnosed with iAMD and 64 (34%) were diagnosed with late non-exudative AMD at baseline. For these 191 eyes, the follow-up ranged from 1 to 47 months, with a mean follow-up of 22 months. Sixteen eyes with subclinical MNV at baseline did not develop exudation during the entire study. Figures 1 and 2 represent two such cases with iAMD that were diagnosed with subclinical MNV at baseline and followed for 27 and 28 months, respectively. The neovascular lesions grew slowly during the follow-up period, but these eyes did not develop any evidence of exudation. Of the 191 eyes that had follow-up visits, 19 eyes developed exudation, which represents a Kaplan-Meier cumulative incidence of exudation of 11.4% at two years. Among these 19 eyes that developed exudation, 13 eyes had subclinical type 1 MNV detected before exudation, one eye had subclinical type 3 MNV before exudation, and five eyes had no prior diagnosis of subclinical MNV before exudation. Overall, of the 191 eyes that had more than one visit, the relative risk of exudation after detection of subclinical

MNV at two years of follow-up was 13.6 times (95% confidence interval, 4.9–37.7) greater than in the absence of subclinical MNV ($P < 0.001$, time-dependent covariate Cox proportional hazards regression).

Of the 19 eyes that developed exudation, subclinical MNV was detected before exudation in 14 eyes. Figures 3 to 6 show eyes that were followed from baseline until they developed exudation and received treatment. The case in figure 3 developed exudation after 24 months of observation and responded well with eight anti-VEGF injections over one year. Figure 4 depicts a case that presented to the emergency room (ER) with symptomatic exudation after 14 months of follow-up. SS-OCTA imaging was missed on the day of injection. In this case, the size of the MNV decreased one month after the first anti-VEGF injection (Fig. 4F). After five anti-VEGF injections over nine months, significant morphological changes were observed (Fig. 4H). Figure 5 shows an eye with a small neovascular lesion that developed exudation after nine months of observation. After the first anti-VEGF treatment, the exudation resolved and the lesion decreased in size, but over the next 16 months and 9 injections, the lesion continued to enlarge. Figure 6 shows subclinical MNV consisting of multiple foci. Two foci in figure 6 developed independent areas of exudation. The lesions responded well to anti-VEGF therapy and the size of the foci remained relatively stable during the next 17 months of follow-up. These cases demonstrate the wide variability of lesion appearance and response before and after anti-VEGF treatment, but in all cases, the macular fluid was successfully managed once exudation developed.

Of the 30 eyes diagnosed with subclinical MNV at the initial SS-OCTA imaging visit, 26 eyes had more than one visit. The Kaplan-Meier method was used to estimate the cumulative incidence of exudation by two years of follow-up. Figure 7 shows the 2-year cumulative incidence of the exudation in eyes with or without MNV at their initial SS-OCTA imaging visit. In eyes with subclinical MNV ($n=26$), the incidence of exudation was 34.5% compared with an incidence of exudation of 6.3% in eyes ($n=165$) without subclinical MNV ($P < 0.001$, log-rank test). Among the 165 eyes without subclinical MNV at the initial SS-OCTA imaging visit, 12 eyes developed subclinical MNV during the follow-up period that ranged from 4 to 30 months. Of these 12 eyes that developed subclinical MNV, 9 eyes had type 1 MNV identified and 3 eyes had early type 3 subclinical MNV. The cumulative incidence of subclinical MNV was 5.5% at 1 year of follow-up and 8.9% at 2 years of follow-up. When calculating the incidence of exudation from the time of the first observation of any subclinical MNV, either at baseline or during follow up, the incidence was 24.2% at the 1 year of follow up, and 34.5% at 2 years of follow-up (Fig 8). There was no difference in the cumulative incidence of exudation from pre-existing MNV in eyes with iAMD or late AMD ($P = 0.540$, log-rank test).

Of the five eyes that demonstrated exudation without prior diagnosis of subclinical MNV, three of them were previously reported in the one-year natural history study.⁷ In this current study, two additional eyes developed exudation without prior detection of subclinical MNV. One of the new exudative cases had not been imaged with SS-OCTA for 12.4 months prior to the onset of exudation. The patient initially declined SS-OCTA imaging, which was performed when the patient returned for routine follow-up for management of the fellow eye that had established exudative disease and required anti-VEGF therapy. Routine clinical SD-

OCT imaging detected the new onset macular fluid on the retinal thickness map and B-scans from this patient. The other case with exudation without prior detection of subclinical MNV was an example in which a precursor of type 3 MNV was missed. Retrospective analysis of the SS-OCTA images revealed hyperreflective foci in the outer retinal layers where the exudation arose, and this exudation was associated with a subtle flow signature suggestive of an angiomatic lesion that was located in the same area where the subsequent intraretinal cystic fluid accumulated.

Due to the evolution of the SS-OCTA prototypes prior to April 2016, continuous growth measurements were problematic because of the differences in scan patterns and signal strength. However, we did explore whether there was a correlation between the size of the lesion immediately prior to exudation and the risk of exudation. We could also assess whether absolute size could serve to predict the need for anti-VEGF therapy. For those eyes that developed exudation, lesion area measurements were obtained at the last two visits prior to exudation. For those eyes that did not develop exudation, we obtained the measurements at the last two visits prior to the final follow-up visit. The sensitivity and specificity of the measurements were assessed by AUROC. The AUROC of the last visit of subclinical MNV was 0.56 (P=0.58), the AUROC of the penultimate visit of subclinical MNV was 0.64 (P=0.28), neither showing discriminable sensitivity nor specificity for predicting exudation. Baseline lesion sizes were evaluated by splitting the lesions into tertiles based on their baseline size: less than 0.082 mm² (32%), between 0.082–0.68 mm² (35%) and larger than 0.68 mm² (32%). These tertiles were compared with the Kaplan-Meier analysis. The result showed that the cumulative proportion of eyes with exudation increased over time in all the different baseline size groups (data not shown), and there were no significant differences among them (P=0.91).

Since there were five eyes that demonstrated exudation without prior diagnosis of subclinical MNV, we wanted to know if poorer surveillance of these eyes could be one of the factors that led to our failure to detect the subclinical MNV prior to exudation. Among cases that developed exudation, we performed a length of visit interval comparison between the five eyes without prior detection of subclinical MNV and the 14 eyes with prior detection of subclinical MNV. The five eyes without subclinical MNV observed had an average interval of 5.9 months (SD=4.7) from the penultimate visit to the anti-VEGF injection, ranging from 1.8 months to 12.4 months, while the cases with prior detection of subclinical MNV had an average interval of 2.7 months (SD=2.6), ranging from 0.2 months to 8.6 months, but this difference was not statistically significant (p=0.073, 2 sample t-test). Similarly, when we compared the overall average visit interval length from baseline to injection in the cases without prior detection of subclinical MNV, the average interval was 5.9 months (SD=4.7), and for cases with subclinical MNV, the average interval was 2.8 months (SD=2.4). Once again, the eyes without subclinical MNV had less frequent follow-up, but this difference was not statistically significant (p=0.065, 2 sample t-test).

DISCUSSION

In this two-year follow-up study of 227 eyes with non-exudative AMD in which the fellow eye had exudative AMD, the overall prevalence of subclinical MNV was 13.2%, which was

similar to the prevalence of 14.4% in 160 eyes from our previous one-year study.⁷ The cumulative incidence rates of new subclinical MNV were also similar between the two studies with 5.4% at one year and 8.9% at two years. However, our subclinical MNV prevalence rates of 13.2% and 14.4% were higher than the 6.25% rate reported by Bailey et al.¹⁹ The lower rate reported by Bailey et al.¹⁹ may be due to the decreased detection of type 1 MNV from their use of SD-OCTA instead of SS-OCTA. Yanagi et al.^{20,21} used SS-OCTA to study the prevalence of unilateral non-exudative MNV in Asian population. They found a 19% prevalence of subclinical MNV and of the 18 patients with subclinical MNV, 10 of the eyes were diagnosed with polypoidal choroidal vasculopathy (PCV). The higher prevalence rate in this Asian study compared with the rate reported by Bailey et al.¹⁹ could also be explained by the use of SS-OCTA, as well as the higher prevalence of exudative PCV in Asian patients,²² which might also result in a higher prevalence of subclinical non-exudative PCV in these eyes.

The important conclusion from our study is that the risk of exudation was greater for eyes with documented subclinical MNV compared with eyes without detectable MNV. The exudation risk for eyes with subclinical MNV increased from 24% after one year of follow-up to 34.5% after 2 years follow up. In our one-year report, the relative risk of exudation after subclinical MNV detection was 15.2 times greater than in eyes without detectable MNV with a 95% confidence interval of 4.2 to 55.4. In the current report, after an additional 67 cases were enrolled, the estimated relative risk of exudation was 13.6 times greater with an increased precision as shown by the narrower confidence interval of 4.9–37.7. The slight decrease in the risk estimate between our previous report and the current one is likely due to chance. We also found that when evaluating non-exudative AMD eyes with either iAMD or GA, there were no differences in the prevalence of subclinical MNV or the cumulative incidence of exudation from preexisting MNV as reported in our previous study.

Of the five eyes that developed exudation without prior detection of subclinical MNV, three of these eyes had not been imaged by SS-OCTA for an extended period of time, one eye was found to contain an unrecognized area of hyperreflective material with detection of a subtle outer retinal angiomatous lesion consistent with an early type 3 neovascular lesion²³ and one eye was found to have a small subclinical neovascular lesion that was missed. The failure to recognize small subclinical MNV is a limitation of the SS-OCTA imaging strategy. Small vascularized drusen can be easily missed, especially when a flow signal associated with a druse might be confused with an artefactual flow signature resulting from overlying retinal vessel projection artifacts.²⁴ Even though projection artifact removal algorithms have improved our ability to identify actual vascularized drusen, some ambiguity persists.^{18,24} Of note, two of the patients with inadequate follow-up were the result of summertime absences and the lack of OCTA capability when followed at the other sites. If these cases had been imaged by SS-OCTA more closely, then we may have been able to detect the formation of a subclinical neovascular lesion before exudation developed. We did find that the length of the average interval between the penultimate visit and the anti-VEGF injection in eyes without subclinical MNV was longer than in eyes with subclinical MNV. The five eyes without subclinical MNV had an average interval of 5.9 months while the 14 cases with subclinical MNV had an average interval of 2.7 months, but this difference was not statistically significant; however, the numbers were small.

The cumulative risk of exudation from subclinical MNV increased to 34.5 % at two years follow up, but the majority of the subclinical lesions continued to grow slowly without exudation up to the longest follow-up period of over 28 months. The reason why some subclinical lesions develop exudation while the others do not is still unknown. We tried to collect consecutive lesion size data and calculate the growth rate of the lesions with the belief that the rate of growth might predict exudation. Unfortunately, due to the evolution of the SS-OCTA technology prior to April 2016, we were unable to calculate reliable continuous growth measurements prior to exudation due to differences in scan patterns and signal strength between the SS-OCTA prototypes. However, we used another strategy and explored whether absolute lesion size could serve to predict the need for anti-VEGF therapy. Our results showed that the lesion size and the likelihood of exudation of subclinical MNV were not related. While we found a small and non-significant reduction in risk associated with larger size during the study, there were only 5 lesions in this study greater than 3.34 mm² at baseline testing and only one of them produced exudation during the follow up. As a result, the number of cases were too small to draw any meaningful statistical conclusion. In another study of eyes with subclinical MNV, Yanagi et al²⁰ observed that enlargement of subclinical MNV may occur before exudation eventually occurs. However, we have found that growth is to be expected over time whether or not exudation develops. Perhaps, the rate of growth could be used as a predictor of future exudation, and we are testing this possibility by accumulating follow-up measurements with the latest SS-OCTA platform to ensure that our growth measurements are reliable. Another possibility is that changes in the blood flow velocity or distribution within subclinical MNV could serve as harbingers of exudation. While our current SS-OCTA instrument cannot perform relative blood flow measurements, the use of variable interscan time analysis (VISTA) for discrimination relative blood flow velocities may prove useful in studying changes in blood flow within these subclinical neovascular lesions as predictors of exudation.^{25–28}

Rather than measuring changes within the MNV, it might be possible to predict the onset of exudation by studying impairment of choriocapillaris blood flow in close proximity to subclinical MNV. A number of studies have reported choriocapillaris flow impairment within the macula associated with AMD in post mortem eyes²⁶ and *in vivo* using SS-OCTA imaging.²⁷ Moulton et al.²⁸ used SS-OCTA imaging to identify focal choriocapillaris flow impairment associated with areas of nascent GA and drusen-associated GA. Recent reports have found similar results and have strengthened the association between choriocapillaris flow impairment associated with both drusen and the progression of GA.^{29,30} In another study, Moulton et al³¹ studied 16 AMD eyes with active neovascularization, 14 of which were surrounded by regions of severe choriocapillaris flow impairment detected by SS-OCTA. Therefore, it seems reasonable to investigate changes in choriocapillaris flow impairment around subclinical MNV, as well as possible changes in lesion volume and changes in the blood flow within the neovascular lesion as potential risk factors for future exudation.

As emphasized in our previous one-year report, we do not recommend the treatment of subclinical MNV with anti-VEGF therapy even when the subclinical lesions are growing. The results from our current two-year study further support this recommendation since the onset of exudation occurs in a minority of cases. We recommend close follow-up and treatment when symptomatic exudation occurs. In our experience, prompt treatment with

anti-VEGF therapy when exudation develops results in improvement and maintenance of visual acuity over two years. As shown in Figures 3 through 6, anti-VEGF therapy results in some lesions shrinking and other lesions growing, but as long as the macula remains fluid free, visual acuity is preserved. We also discourage treatment in the absence of exudation because of the potential effects of anti-VEGF therapy on a non-exudative lesion. These non-exudative lesions may be the body's attempt to recapitulate the choriocapillaris closer to the RPE and this neovascularization may serve a vital nutritional support function for the RPE.³² Therefore, elimination of the subclinical neovascularization by anti-VEGF therapy may accelerate the formation of macular atrophy. Moreover, if treatment of a nonexudative lesion is initiated, then when would the treatment be stopped? The endpoint for anti-VEGF therapy is usually the elimination of exudation and if there was no exudation at the start of treatment, then when would the anti-VEGF therapy ever be stopped since most type 1 neovascular lesions do not regress after anti-VEGF therapy. As a result, if anti-VEGF therapy is initiated, then the clinician will be treating until GA develops. Considering the costs, risks, and benefits of anti-VEGF therapy, we recommend close observation and home monitoring as the best strategy for management of treatment-naïve asymptomatic subclinical neovascular lesions.

One of the limitations of this study includes the variable follow-up intervals, which were determined based on the need for anti-VEGF therapy in the fellow eye that had exudative AMD. Since exudation may have preceded the onset of visual complaints, and the interval between the onset of exudation and the date of anti-VEGF therapy depended on the patients' visual complaints, we used the visit when the patient received treatment with intravitreal anti-VEGF therapy as the day of symptomatic exudation rather than the day when macular fluid first developed. Another limitation of this study was with the use of three different SS-OCTA prototypes. This limited our ability to reliably measure the continuous growth rate of the neovascular lesion. Therefore, we focused on the influence of subclinical neovascular lesion sizes at the last two visits to assess whether there was an association with exudation. We did not find a correlation between lesion size and exudation, which is an important observation given the fact that clinicians will discover these lesions incidentally, and now we know that all lesions should be followed closely for exudation regardless of size.

In summary, SS-OCTA is a safe, fast, noninvasive strategy to diagnose and monitor subclinical MNV in asymptomatic eyes with non-exudative AMD. By two years of follow up, the cumulative exudation risk was 13.6 times greater in eyes diagnosed with subclinical MNV compared with eyes without detectable lesions and the size of the lesion does not appear to be a risk factor in developing exudation. We recommend that patients with subclinical MNV be monitored more frequently, and the use of home monitoring would be ideal for this population. Further prospective studies are needed to investigate whether changes in perilesional choriocapillaris blood flow, total lesion volume, and lesion blood flow velocity may predict a future risk of exudation.

ACKNOWLEDGMENTS/DISCLOSURES:

a. Funding/Support: Research supported by grants from Carl Zeiss Meditec, Inc. (Dublin, CA), the National Eye Institute (R01EY024158, R01EY028753), the Salah Foundation, the National Eye Institute Center Core Grant

(P30EY014801) and Research to Prevent Blindness (unrestricted Grant) to the Department of Ophthalmology, University of Miami Miller School of Medicine.

b. Financial Disclosures: Giovanni Gregori, Ruikang K. Wang and Philip J. Rosenfeld received research support from Carl Zeiss Meditec, Inc. Giovanni Gregori and the University of Miami co-own a patent that is licensed to Carl Zeiss Meditec, Inc. Philip J. Rosenfeld also received additional research support from Genentech. He is a consultant for Apellis, Boehringer-Ingelheim, Carl Zeiss Meditec, Chengdu Kanghong Biotech, Oculunex Therapeutics, Healios K.K, Hemera Biosciences, F. Hoffmann-La Roche Ltd., Isarna Pharmaceuticals, Oculunex, Oculdyne, and Unity Biotechnology. Philip J. Rosenfeld has equity interest in Apellis, Verana Health, and Oculdyne. Ruikang K. Wang discloses intellectual property owned by the Oregon Health and Science University and the University of Washington related to OCT angiography, and licensed to commercial entities, which are related to the technology and analysis methods described in parts of this manuscript. Ruikang K. Wang also receives research support from Colgate-Palmolive Company, Moptim Inc, and Facebook Technologies, LLC. He is a consultant to Insight Photonic Solutions, and Kowa.

Luis de Sisternes and Mary K. Durbin are employed by Carl Zeiss Meditec, Inc. Jin Yang, Qinqin Zhang, Elie H. Motulsky, Marie Thulliez, Yingying Shi, Cancan Lyu and William Feuer have no disclosures. All authors attest that they meet the current ICMJE criteria for authorship.

c. Other Acknowledgments: None

REFERENCES

1. Comparison of Age-related Macular Degeneration Treatments Trials Research G, Martin DF, Maguire MG, et al. Ranibizumab and bevacizumab for treatment of neovascular age-related macular degeneration: two-year results. *Ophthalmology*. 2012;119(7):1388–1398. [PubMed: 22555112]
2. Jaffe GJ, Ying GS, Toth CA, et al. Macular Morphology and Visual Acuity in Year Five of the Comparison of Age-related Macular Degeneration Treatments Trials. *Ophthalmology*. 2019;126(2):252–260. [PubMed: 30189282]
3. Schneider U, Gelissen F, Inhoffen W, Kreissig I. Indocyanine green angiographic findings in fellow eyes of patients with unilateral occult neovascular age-related macular degeneration. *Int Ophthalmol*. 1997;21(2):79–85. [PubMed: 9405989]
4. Hanutsaha P, Guyer DR, Yannuzzi LA, et al. Indocyanine-green videoangiography of drusen as a possible predictive indicator of exudative maculopathy. *Ophthalmology*. 1998;105(9):1632–1636. [PubMed: 9754169]
5. Querques G, Srouf M, Massamba N, et al. Functional characterization and multimodal imaging of treatment-naïve “quiescent” choroidal neovascularization. *Invest Ophthalmol Vis Sci*. 2013;54(10):6886–6892. [PubMed: 24084095]
6. Guyer DR, Yannuzzi LA, Slakter JS, et al. Classification of choroidal neovascularization by digital indocyanine green videoangiography. *Ophthalmology*. 1996;103(12):2054–2060. [PubMed: 9003339]
7. de Oliveira Dias JR, Zhang Q, Garcia JMB, et al. Natural History of Subclinical Neovascularization in Nonexudative Age-Related Macular Degeneration Using Swept-Source OCT Angiography. *Ophthalmology*. 2018;125(2):255–266. [PubMed: 28964581]
8. Roisman L, Zhang Q, Wang RK, et al. Optical Coherence Tomography Angiography of Asymptomatic Neovascularization in Intermediate Age-Related Macular Degeneration. *Ophthalmology*. 2016;123(6):1309–1319. [PubMed: 26876696]
9. Miller AR, Roisman L, Zhang Q, et al. Comparison Between Spectral-Domain and Swept-Source Optical Coherence Tomography Angiographic Imaging of Choroidal Neovascularization. *Invest Ophthalmol Vis Sci*. 2017;58(3):1499–1505. [PubMed: 28273316]
10. Zhang Q, Chen CL, Chu Z, et al. Automated Quantitation of Choroidal Neovascularization: A Comparison Study Between Spectral-Domain and Swept-Source OCT Angiograms. *Invest Ophthalmol Vis Sci*. 2017;58(3):1506–1513. [PubMed: 28273317]
11. Novais EA, Adhi M, Moulton EM, et al. Choroidal Neovascularization Analyzed on Ultrahigh-Speed Swept-Source Optical Coherence Tomography Angiography Compared to Spectral-Domain Optical Coherence Tomography Angiography. *Am J Ophthalmol*. 2016;164:80–88. [PubMed: 26851725]

12. Ferris FL 3rd, Wilkinson CP, Bird A, et al. Clinical classification of age-related macular degeneration. *Ophthalmology*. 2013;120(4):844–851. [PubMed: 23332590]
13. Huang Y, Zhang Q, Thorell MR, et al. Swept-source OCT angiography of the retinal vasculature using intensity differentiation-based optical microangiography algorithms. *Ophthalmic Surg Lasers Imaging Retina*. 2014;45(5):382–389. [PubMed: 25230403]
14. Wang RK, An L, Francis P, Wilson DJ. Depth-resolved imaging of capillary networks in retina and choroid using ultrahigh sensitive optical microangiography. *Opt Lett*. 2010;35(9):1467–1469. [PubMed: 20436605]
15. Zheng F, Zhang Q, Motulsky EH, et al. Comparison of Neovascular Lesion Area Measurements From Different Swept-Source OCT Angiographic Scan Patterns in Age-Related Macular Degeneration. *Invest Ophthalmol Vis Sci*. 2017;58(12):5098–5104. [PubMed: 28986595]
16. Zhang Q, Wang RK, Chen CL, et al. Swept Source Optical Coherence Tomography Angiography of Neovascular Macular Telangiectasia Type 2. *Retina*. 2015;35(11):2285–2299. [PubMed: 26457402]
17. Zhang A, Zhang Q, Wang RK. Minimizing projection artifacts for accurate presentation of choroidal neovascularization in OCT micro-angiography. *Biomed Opt Express*. 2015;6(10):4130–4143. [PubMed: 26504660]
18. Zhang Q, Zhang A, Lee CS, et al. Projection artifact removal improves visualization and quantitation of macular neovascularization imaged by optical coherence tomography angiography. *Ophthalmol Retina*. 2017;1(2):124–136. [PubMed: 28584883]
19. Palejwala NV, Jia Y, Gao SS, et al. Detection of Nonexudative Choroidal Neovascularization in Age-Related Macular Degeneration with Optical Coherence Tomography Angiography. *Retina*. 2015;35(11):2204–2211. [PubMed: 26469533]
20. Yanagi Y, Mohla A, Lee SY, et al. Incidence of Fellow Eye Involvement in Patients With Unilateral Exudative Age-Related Macular Degeneration. *JAMA Ophthalmol*. 2018;136(8):905–911. [PubMed: 29879284]
21. Yanagi Y, Mohla A, Lee WK, et al. Prevalence and Risk Factors for Nonexudative Neovascularization in Fellow Eyes of Patients With Unilateral Age-Related Macular Degeneration and Polypoidal Choroidal Vasculopathy. *Invest Ophthalmol Vis Sci*. 2017;58(9):3488–3495. [PubMed: 28702676]
22. Wong CW, Yanagi Y, Lee WK, et al. Age-related macular degeneration and polypoidal choroidal vasculopathy in Asians. *Prog Retin Eye Res*. 2016;53:107–139. [PubMed: 27094371]
23. Nagiel A, Sarraf D, Sadda SR, et al. Type 3 neovascularization: evolution, association with pigment epithelial detachment, and treatment response as revealed by spectral domain optical coherence tomography. *Retina*. 2015;35(4):638–647. [PubMed: 25650713]
24. Zheng F, Roisman L, Schaal KB, et al. Artfactual Flow Signals Within Drusen Detected by OCT Angiography. *Ophthalmic Surg Lasers Imaging Retina*. 2016;47(6):517–522. [PubMed: 27327280]
25. Ploner SB, Moulton EM, Choi W, et al. TOWARD QUANTITATIVE OPTICAL COHERENCE TOMOGRAPHY ANGIOGRAPHY: Visualizing Blood Flow Speeds in Ocular Pathology Using Variable Interscan Time Analysis. *Retina*. 2016;36 Suppl 1:S118–S126. [PubMed: 28005670]
26. Biesemeier A, Taubitz T, Julien S, Yoeruek E, Schraermeyer U. Choriocapillaris breakdown precedes retinal degeneration in age-related macular degeneration. *Neurobiol Aging*. 2014;35(11):2562–2573. [PubMed: 24925811]
27. Moreira-Neto CA, Moulton EM, Fujimoto JG, Waheed NK, Ferrara D. Choriocapillaris Loss in Advanced Age-Related Macular Degeneration. *J Ophthalmol*. 2018;2018:8125267. [PubMed: 29651346]
28. Moulton EM, Waheed NK, Novais EA, et al. Swept-Source Optical Coherence Tomography Angiography Reveals Choriocapillaris Alterations in Eyes with Nascent Geographic Atrophy and Drusen-Associated Geographic Atrophy. *Retina*. 2016;36 Suppl 1:S2–S11. [PubMed: 28005659]
29. Nassisi M, Shi Y, Fan W, et al. Choriocapillaris impairment around the atrophic lesions in patients with geographic atrophy: a swept-source optical coherence tomography angiography study. *Br J Ophthalmol*. 2018.
30. Borrelli E, Shi Y, Uji A, et al. Topographic Analysis of the Choriocapillaris in Intermediate Age-related Macular Degeneration. *Am J Ophthalmol*. 2018;196:34–43. [PubMed: 30118688]

31. Moulton E, Choi W, Waheed NK, et al. Ultrahigh-speed swept-source OCT angiography in exudative AMD. *Ophthalmic Surg Lasers Imaging Retina*. 2014;45(6):496–505. [PubMed: 25423628]
32. Grossniklaus HE, Green WR. Choroidal neovascularization. *Am J Ophthalmol*. 2004;137(3):496–503. [PubMed: 15013874]

Author Manuscript

Author Manuscript

Author Manuscript

Author Manuscript

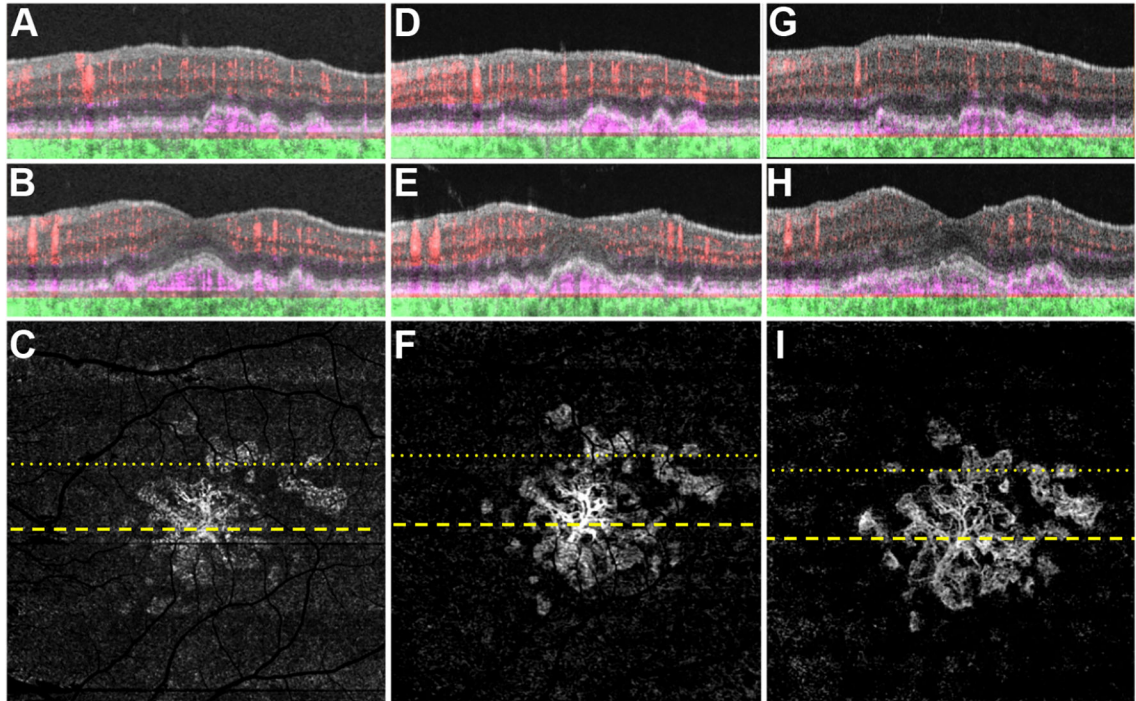


FIGURE 1.

Swept source optical coherence tomography angiography (SS-OCTA) 6×6 mm scans of the asymptomatic eye from a patient with exudative AMD in the fellow eye, followed for 27 months without exudation. (**A,B,D,E,G,H**) SS-OCTA B-scans with color-coded flow, where red represents the retinal microvasculature, pink the outer retina-tochoriocapillaris (ORCC) slab, and green the remainder of the choroid. The pink coloration under the retinal pigment epithelium and above Bruch's membrane represents the type 1 macular neovascularization. (**A,D,G**) SS-OCTA B-scans superior to the fovea (dotted line in C,F,I). (**B,E,H**) SS-OCTA B-scans through the fovea (dashed line in C,F,I). (**C,F,I**) SS-OCTA *en face* ORCC slab images, after removal of retinal vessel projection artifacts. (**C**) SS-OCTA *en face* ORCC slab image showing a multilobular and multifocal neovascular complex with a total area of 4.70 mm². (**D-F**) Images obtained 14 months after those in (A-C). (**F**) SS-OCTA *en face* ORCC slab image showing a multilobular and multifocal neovascular complex with a total area of 5.11 mm². (**G-I**) Images obtained 13 months after those in (D-F). (**I**) SS-OCTA *en face* ORCC slab image showing a multilobular and multifocal neovascular complex with a total area of 5.90 mm².

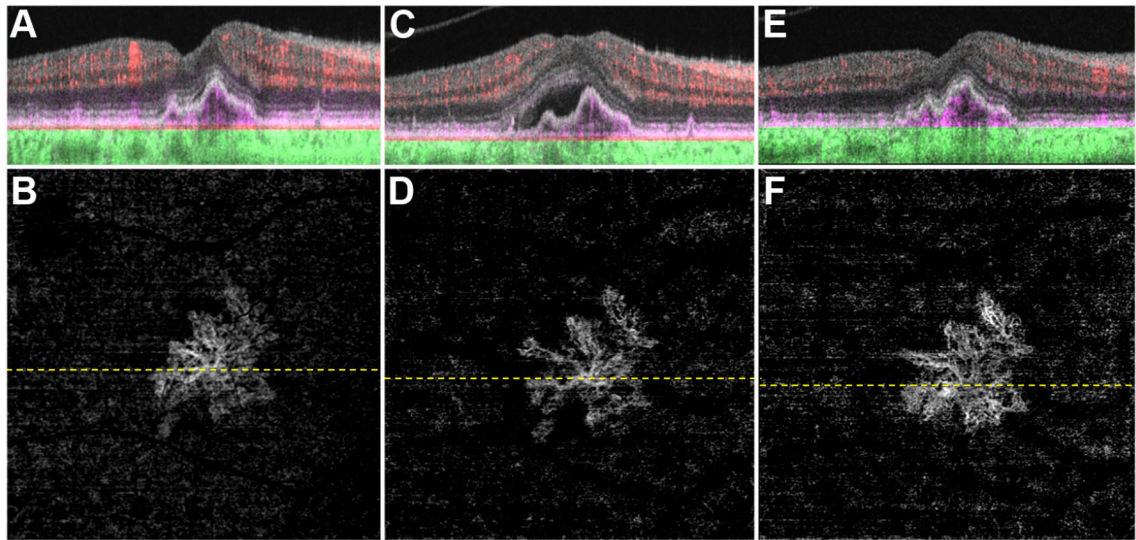


FIGURE 2.

Swept source optical coherence tomography angiography (SS-OCTA) 6×6 mm scans of the asymptomatic eye from a patient with exudative AMD in the fellow eye followed up for 28 months without exudation. (A,C,E) SS-OCT B-scan through the fovea with color-coded flow, where red represents the retinal microvasculature, pink the outer retina-to-choriocapillaris (ORCC) slab, and green the remainder of the choroid. The pink coloration under the retinal pigment epithelium and above Bruch's membrane, which represents the type 1 macular neovascularization. (B,D,F) SS-OCTA *en face* ORCC slab images, after removal of retinal vessel projection artifacts. The dashed line represents the B-scan contained in (A,C,E). (B) SS-OCTA *en face* ORCC slab image showing a wreath-shaped neovascular complex with a total area of 7.10 mm². (C, D) Images obtained 14 months after those in (A, B). (D) SS-OCTA *en face* ORCC slab image showing a wreath-shaped neovascular complex with a total area of 7.39 mm². (E, F) Images obtained 14 months after those in (C, D). (F) SS-OCTA *en face* ORCC slab image showing a wreath-shaped neovascular complex with a total area of 7.91 mm².

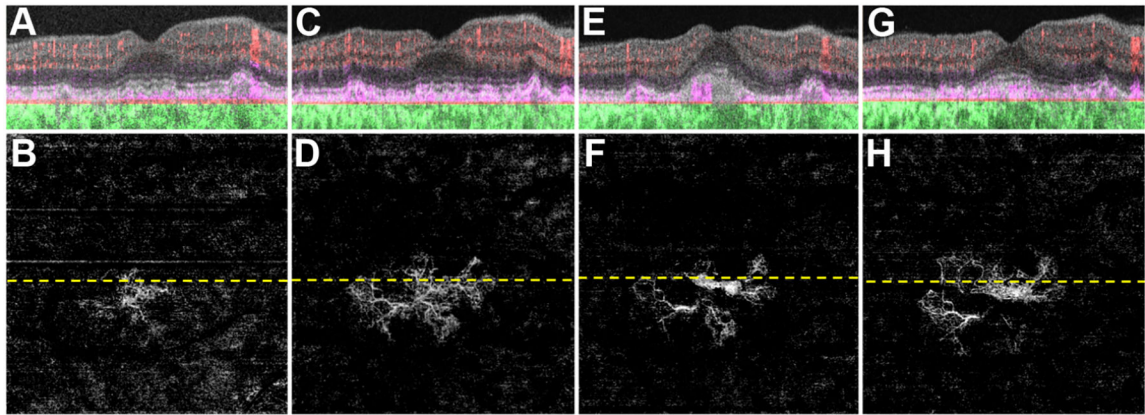


FIGURE 3.

Swept-source optical coherence tomography angiography (SS-OCTA) 6×6mm scans of the asymptomatic eye from a patient with exudative AMD in the fellow eye followed up for 36 months in which exudation developed requiring aflibercept therapy after 24 months of observation. (A,C,E) SS-OCTA B-scan through the fovea with color-coded flow, where red represents the retinal microvasculature, pink the outer retina-to-choriocapillaris (ORCC) slab, and green the remainder of the choroid. The pink coloration under the retinal pigment epithelium and above Bruch's membrane, which represents the type 1 macular neovascularization. (B,D,F) SS-OCTA *en face* ORCC slab image, after removal of retinal vessel projection artifacts. The dashed line represents the B-scan contained in (A,C,E). (B) SS-OCTA *en face* ORCC slab image showing a multilobular neovascular complex with a total area of 2.42 mm². (C, D) Images obtained 3 months after those in (A, B). (C) SS-OCTA B-scan with color-coded flow through the fovea showing subretinal fluid through the fovea. (D) SS-OCTA *en face* ORCC slab image showing a neovascular lesion with an area of 2.88 mm². (E, F) Images obtained 12 months after those in (C, D). (E) SS-OCTA B-scan with color-coded flow through the fovea showing resolved subretinal fluid after eight anti-VEGF injections. (F) SS-OCTA *en face* ORCC slab image showing a neovascular lesion with an area of 2.75 mm². After anti-VEGF therapy, no significant change in the configuration of the MNV was appreciated.

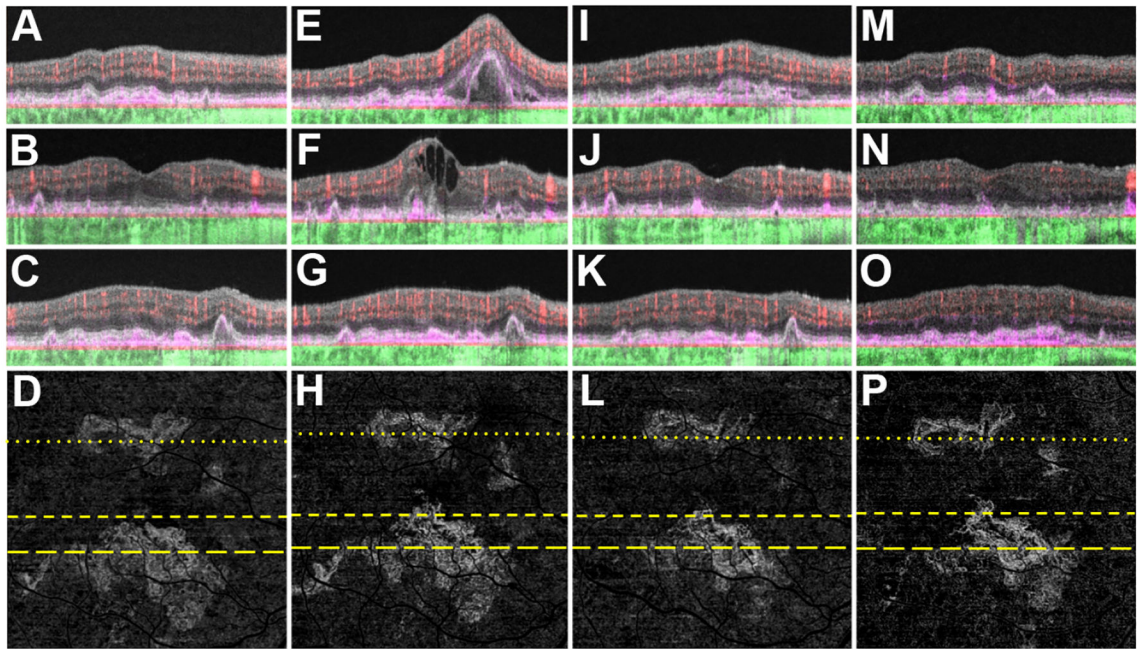


FIGURE 4.

Swept source optical coherence tomography angiography (SS-OCTA) 6×6 mm scans of the asymptomatic eye from a patient with exudative AMD in the fellow eye followed up for 25 months in which exudation developed requiring anti-VEGF therapy after 14 months of observation. (A,C,E,G) SS-OCTA B-scan through the fovea with color-coded flow, where red represents the retinal microvasculature, pink the outer retina-to-choriocapillaris (ORCC) slab, and green for the remainder of the choroid. The pink coloration under the retinal pigment epithelium and above Bruch's membrane, which represents the type 1 macular neovascularization. (B,D,F,H) SS-OCTA *en face* ORCC slab image, after removal of retinal vessel projection artifacts. The dashed line represents the B-scan contained in (A,C,E,G). (B) SS-OCTA *en face* ORCC slab image showing a multilobular neovascular complex with a total area of 0.69 mm². (C, D) Images obtained 13 months after those in (A, B). (D) SS-OCTA *en face* ORCC slab image showing a neovascular lesion with an area of 2.97 mm². Because of the patient was symptomatic with subretinal fluid presented two months after those in (C, D), the patient received anti-VEGF therapy in the ER, so the SS-OCTA imaging was not performed on the day of injection. (E, F) Images obtained one month after the first injection. (E) SS-OCTA B-scan with color-coded flow through the fovea showing the treated type 1 macular neovascularization. (F) SS-OCTA *en face* ORCC slab image showing a neovascular lesion with an area of 2.51 mm². (G, H) Images obtained 9 months after those in (E, F). (G) SS-OCTA B-scan with color-coded flow through the fovea showing decreased RPE elevation after five anti-VEGF injections. (H) SS-OCTA *en face* ORCC slab image showing a neovascular lesion with a total area of 3.21 mm².

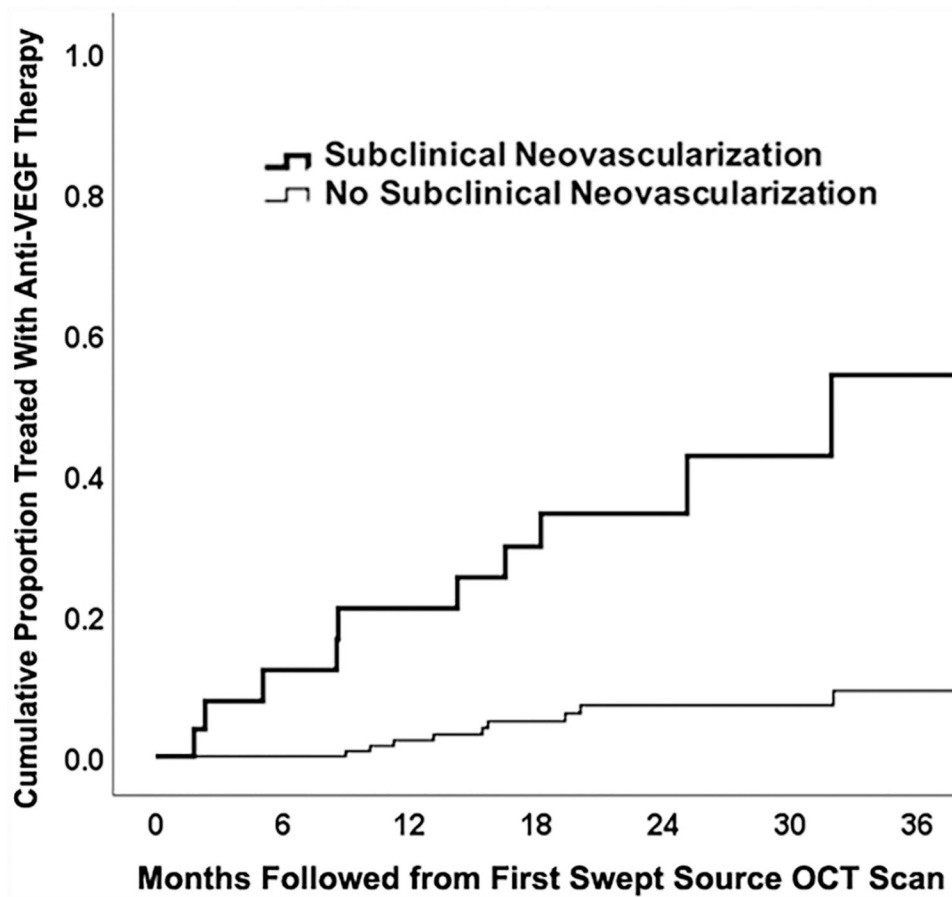


FIGURE 5.

Swept source optical coherence tomography angiography (SS-OCTA) 3×3 mm scans of the asymptomatic eye from a patient with exudative AMD in the fellow eye followed up for 26 months in which exudation developed requiring anti-VEGF therapy after 9 months of observation. (A,C,E,G) SS-OCTA B-scan through the fovea with color-coded flow, where red represents the retinal microvasculature, pink the outer retina-tochoriocapillaris (ORCC) slab, and green the remainder of the choroid. The pink coloration under the retinal pigment epithelium and above Bruch's membrane, which represents the type 1 macular neovascularization. (B,D,F,H) SS-OCTA *en face* ORCC slab image, after removal of retinal vessel projection artifacts. The dashed line represents the B-scan contained in (A,C,E,G). (B) SS-OCTA *en face* ORCC slab image showing a small lesion with a total area of 0.06 mm²(arrow). (C, D) Images obtained 9 months after those in (A, B). (C) SS-OCTA B-scan with color-coded flow through the fovea and subretinal fluid presented. (D) SS-OCTA *en face* ORCC slab image showing increased neovascular lesion with an area of 0.18 mm². The patient was symptomatic at this visit and intravitreal aflibercept was injected. (E, F) Images obtained 1 month after the first injection. (E) SS-OCTA B-scan with color-coded flow through the fovea showing subretinal fluid resolved. (F) SS-OCTA *en face* ORCC slab image showing a decreased neovascular lesion size with an area of 0.04 mm². (G, H) Images obtained 16 months after those in (E, F). (G) SS-OCTA B-scan with color-coded flow through the fovea still showing the type1 neovascularization after nine anti-VEGF injections.

(H) SS-OCTA *en face* ORCC slab image showing a neovascular lesion extends to an area of 0.11 mm².

Author Manuscript

Author Manuscript

Author Manuscript

Author Manuscript

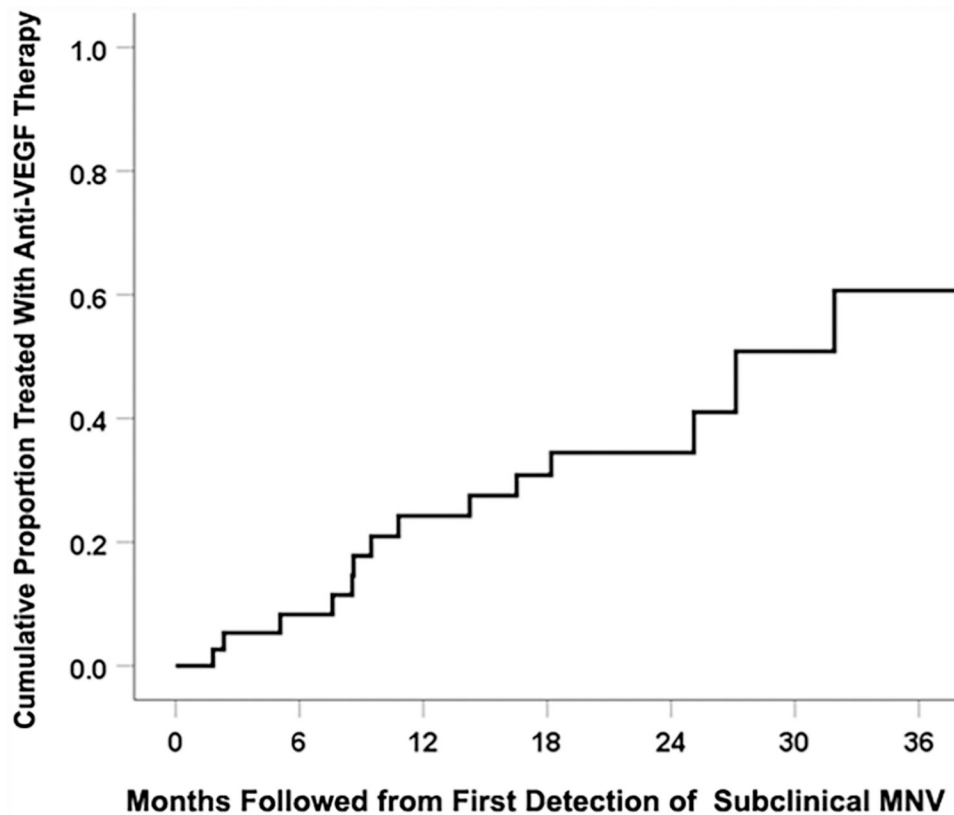


FIGURE 6.

Swept source optical coherence tomography angiography (SS-OCTA) 6×6 mm scans of the asymptomatic eye from a patient with non-exudative AMD in one eye and exudative AMD in the fellow eye followed up for 21 months in which exudation from both of the two neovascular foci developed after 5 months of observation. (A,B,C,E,F,G,I,J,K,M,N,O) SS-OCTA B-scans with color-coded flow represented as red for the retinal microvasculature, pink for the outer retina-to-choriocapillaris (ORCC) slab, and green for the remainder of the choroid. The pink coloration under the retinal pigment epithelium and above Bruch's membrane represents the type 1 macular neovascularization. (A,E,I,M) SS-OCTA B-scans of the first neovascular foci superior to the fovea (dotted line in D,H,L,P). (B,F,J,N) through the second neovascular foci in the foveal (short dashed line in D,H,L,P), (C,G,K,O) through the second neovascular foci inferior to the foveal (long dashed line in D,H,L,P), (D) SS-OCTA *en face* ORCC slab image showing MNV with a total area of 5.32 mm². (E-H) Images obtained 5 months after those in (A-D). (E,F) B-scans of the both of the neovascular foci appears to be associated with new onset exudation. (H) SS-OCTA *en face* ORCC slab image showing the MNV with a total area of 6.61 mm². The patient was symptomatic at that visit and intravitreal aflibercept was given. (I-L) Images obtained 1 month after the exudation, those in (E-H). (L) SS-OCTA *en face* ORCC slab image showing the MNV with a total area of 4.19 mm². (M-P) Images obtained 15 months after those in (I-L) after ten anti-VEGF injections. (P) SS-OCTA *en face* ORCC slab image showing the MNV with a total area of 5.49 mm².

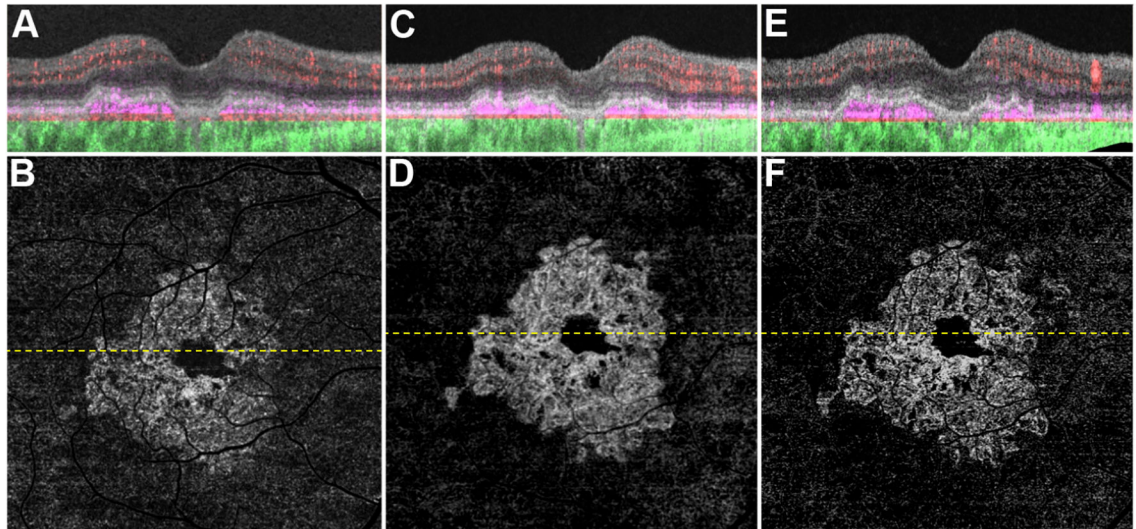


FIGURE 7.

Kaplan-Meier analysis showing the cumulative proportion of eyes treated with anti-vascular endothelial growth factor (VEGF) therapy from the time of the first swept source optical coherence tomography angiography (SS-OCTA). For eyes with subclinical macular neovascularization (MNV) at the time of first SS-OCTA imaging, the incidence of exudation was 21.1% by 12 months and 34.5% by 24 months. For eyes without subclinical MNV at the time of first SS-OCTA imaging, the incidence of exudation was 3.6% by 12 months and 6.3% by 24 months.

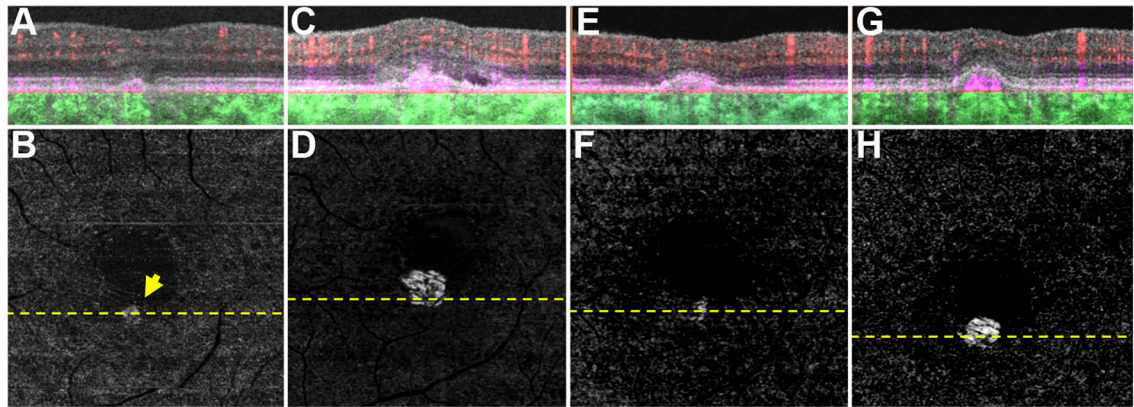


FIGURE 8.

Kaplan-Meier analysis of the cumulative proportion of eyes treated with anti-vascular endothelial growth factor (VEGF) therapy from the time the subclinical macular neovascularization (MNV) was first detected. The overall incidence of exudation from detection of any subclinical MNV was 24.2% by 12 months and 34.5% by 24 months.